ACS Biomaterials SCIENCE & ENGINEERING
Article
Cite This: ACS Biomater. Sci. Eng. 2018, 4, 502−513

Characterization of Nanoscale Loaded Liposomes Produced by 2D Hydrodynamic Flow Focusing

Selya Amrani[†] and Maryam Tabrizian*[,†,‡]

[†]Biomedical Engineering Department-Faculty of Medicine, [‡]Faculty of Dentistry, McGill University, Montreal, Quebec H3A 2B4, Canada

Supporting Information

ABSTRACT: This paper presents the continuous flow formation by two-dimensional (2D) hydrodynamic flow focusing (HFF) of nanosized liposomes in microfluidic systems. The size distribution and concentration of the nanosized liposomes, as well as the polydispersity index (PDI) and zeta potential (ZP) of the liposomal dispersions, were investigated under various flow rate ratios (FRRs) and lipid formulations, by the selective incorporation of either positively charged DDAB (didodecyl-dimethylammonium bromide) or negatively charged DOPG (1,2 dioleoyl-*sn*-glycero-3- phosphoglycerol) lipids to the main bilayer DPPC (1,2-dipalmitoyl-*sn*-glycero-3-phosphocholine) constituent. The challenges of encapsulating an FITC (fluorescein isothiocyanate)-labeled LC-TAT peptide (long chain of transactivator of transcription peptide), which plays a direct role in the HIV regulation and transcription, overcame and could be achieved via one-step nanoliposomes synthesis, in order to validate the potential of this device as an all-in-one nanoparticle synthesis and loading platform. Liposomes with sizes ranging between 60 to 800 nm were produced with low polydispersity and high particle throughput from alteration of the flow rate ratio and lipid concentration. We introduced the use of nanoparticle tracking analysis (NTA) to estimate for the first time the throughput of microfluidic synthesized liposomal NPs by measuring quantitatively the concentration of the synthesized particles at the outlet. These measurements showed that stable and unilamellar liposomes are generated at a maximum concentration of 1740×10^8 particles/mL in less than 2 min, with higher FRR enabling the most rapid generation of liposomes with similar diameter and significant lower polydispersity index than those obtained by other batch techniques.

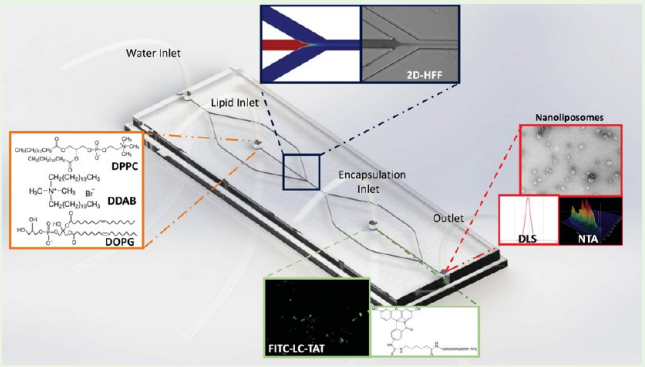

KEYWORDS: *continuous flow microfluidics, nanolipsomes fabrication, passive encapsulation, nanoparticle tracking analysis*

INTRODUCTION

Compared to their nonorganic nanoparticles (NPs) counterparts, the use of liposomes as a delivery vehicle offers many advantages including longer circulation times within the body,[1,2] protection and controlled release of the encapsulated molecules,[3,4] and the ability to overcome biological barriers to achieve targeted delivery.[5,6] Traditional bulk methods of NPs preparation are, however, limited by difficulty in controlling size,[7,8] scaling-up,[9−12] and inconsistent encapsulation efficiency,[13−15] along with difficulty in effective sterilization.[16] In addition, long processing times, difficulty in obtaining relatively monodisperse products, large reagent volumes,[17] and the multiple and lengthy steps necessary for encapsulation,[18−20] make bulk synthesis methods time-consuming and uneconomical.[21,22]

The production of nano/microsized liposomes continues to rely mostly on the formation of a dried lipid film,[23,24] the hydration of which resulting in the self-assembly of lipids in a bulk phase.[1,25,26] Thin-film hydration,[27−29] ethanol injection,[30−33] and detergent dialysis methods[34,35] are all examples of such processes where the self-assembly of lipid vesicles typically occurs under an environment with characteristic dimension of millimeters or centimeters.[36] This leads to local concentration fluctuations of lipids and payloads,[36] and the resultant liposomes are polydispersed in size and often multilamellar. Further postprocessing by extrusion,[27,28] freeze−thaw,[15,37,38] sonication,[28] and/or high-pressure homogenization[36,37] is required, in order to obtain liposomes with specific size and conformations.[39]

In the search for new strategies to alleviate the current issues facing liposome fabrication, modern industrial-grade liposomal fabrication techniques have emerged which provide high amounts of stable homogeneous liposomal formulations and high trapping efficiency.[38] These include processes such as dense gas (DG),[22] high-pressure homogenization (HPH),[40,41] and dual asymmetric centrifugation (DAC).[42] However, these

Received: August 14, 2017
Accepted: January 4, 2018
Published: January 4, 2018

DOI: 10.1021/acsbiomaterials.7b00572
ACS Biomater. Sci. Eng. 2018, 4, 502−513

techniques require multiple stages to achieve the desired final size of liposomes,[41] often operate under high pressures that can readily block nozzles,[22] require high capital costs and cumbersome equipment,[43] or encounter either sterilization issues or difficulties in removing organic solvent residues.[22,41] In this context, drug-loaded nanoliposomes can be produced in one step only with a microfluidic continuous process hold many advantages over current methods. This includes reducing the use of organic solvents, as well as providing fast, low-cost, single-stage production and producing stable, uniform liposomes without the need of extensive postprocessing operations.[36,44]

Jahn et al.[25,26] first reported the controlled synthesis of submicrometer-sized liposomes through microfluidic flow focusing by convective-diffusive mixing, yielding relatively high liposome concentrations and stable liposomes along the interfacial region.[36] A controlled microfluidic mixing and nanoparticle determination platform (COMMAND)[45] was notably used to enable the formation of unilamellar lipid vesicles (liposomes) with diameters of tens of nanometers. Detailed investigations of deterministic liposome formation by controlled microfluidic mixing were concomitantly conducted to investigate the dependence of liposome size distribution on microfluidic device geometry, hydrodynamic flow focusing, and volumetric flow rate.[45] It was demonstrated that liposome size distribution was dependent on several parameters including the device geometry and scaling, the flow rate ratio (FRR), and the total flow rate (TFR).[45] Since then, several flow focusing microfluidic devices have been developed for the production of micro/nanoscale lipid-based vesicular systems,[46−49] with efforts being deployed to further define the parameters determining particle size distribution of the liposomal preparation. The effect of microfluidic chip design and lipid formulations were notably evaluated by Carugo et al.[50] in terms of the size and homogeneity of the end product, where the role of lipid formulation and concentration (including the residual amount of solvent), production method and drug loading was evaluated in determining liposome characteristics.[50] Devices displaying scaled-up versions of microscale flow focusing architectures in the millimeter range were also introduced, to study the scaled-up effect of operating parameters (especially the FRR) on liposomes dimensions.[50] However, while a variety of techniques for liposome synthesis have been reported that take advantage of microfluidic flow elements to achieve precise control over the size and polydispersity of nanoscale liposomes, these methods suffer from extremely limited throughput, making them impractical for large-scale nanoparticle synthesis.[46] As an alternative to enhance the throughput of microfluidic liposome synthesis, studies have been developed which exploited planar 2D HFF microfluidic devices with variable aspect-ratios for nanoscale liposome formation[51] or vertical flow focusing[46] to attempt to overcome the throughput limits of established microfluidic nanoparticle synthesis techniques.[46] Notably, vertical flow focusing technique was utilized by Hood et al.[46] to generate populations of small, unilamellar, and nearly monodisperse liposomal nanoparticles with exceptionally high production rates and sample homogeneity.[46]

Building upon previous HFF work,[43] in which we developed a double flow-focusing microfluidic geometry capable of subhour synthesis and controlled loading of DSPC tunable liposomes, this new platform addresses some of the issues previously encountered with the last prototype, including low particle yield and diluted liposomal solutions at the outlet.[43]

In this work, we therefore address the high throughput synthesis of liposomal particles bellow the 500 nm range without compromising the final particle concentration at the outlet. The through-put of microfluidic devices is typically expressed in terms of mg per minute, which yields limited information as to the particle count/concentration of liposomes in solution.[13,18,52]

A range of instrumentation techniques have been used to characterize the size or concentration of liposome dispersions.[53,54] Multi-angle (static) and dynamic light scattering (MALS and DLS, respectively), used to quantify particles size and charge, although not destructive techniques, are unable to quantify particle concentration and suffer from poor resolution.[55] Separation techniques, such as disc centrifugation (DC) and field-flow fractionation (FFF), do not measure particle charge or concentration, and have separation-based issues.[54] In contrast, particle-by-particle counting techniques, such as tunable resistive pulse sensoring (TRPS) and nanoparticle tracking analysis (NTA), have the advantage of measuring and collating the properties of individual liposomes to direct measurement of the particle concentration with a high resolution and more accurate analysis of the particle size and/or charge (zeta-potential) distribution.[53] However, in the case of TRPS, quantification of liposomes is strongly related to the lower detection limit a parameter that may be unknown for liposomes, thereby resulting in underestimation of their concentration.[56] Liposome samples are also typically destroyed in the process of measuring their concentration, precluding their use in applications requiring real-time monitoring.[57,58] As such, this work attempts to estimate quantitatively by NTA the throughput of hydrodynamic flow-focusing microfluidic devices for liposome formation expressed in terms of the concentration of the produced liposome nanoparticles. Using DPPC as the main bilayer constituent, particle diameters and concentrations were evaluated with respect to phospholipid concentration, composition and flow rates. The effect of these parameters including the FRR and lipid concentration on the size of liposomal vesicles has already been established in the literature,[25,26,45,50] but has to our knowledge never been investigated using the NTA technique. Furthermore, through the addition of different weight ratios of either positively or negatively charged lipid particles to the bilayer DPPC constituent via incorporation of DDAB and DOPG respectively, the effect of lipid charge and colloidal stability on liposome size is also investigated at different FRRs. Understanding how the lipid composition such as the charge could affect microfluidic-based liposomal synthesis and using NTA to estimate the throughput of the microfluidic device are the two main objectives of this study. Finally, as a demonstration of the generality of the microfluidic mixing encapsulation process, encapsulation of a bioactive molecule; a FITC labeled LC-TAT cell-penetrating peptide is also demonstrated. TAT (Trans-Activator of Transcription) is a protein encoded for by the TAT gene in HIV-1 and stimulates HIV-1 gene expression during transcription initiation and elongation.[59] In addition, by antagonizing the CXCR4 receptor, reports suggest that TAT selectively encourage the reproduction of less-virulent M-tropic (macrophage-tropic) strains of HIV early in the course of infection, allowing the more rapidly pathogenic T-cell-tropic strains that use the CXCR4 receptor to emerge later after mutating from M-tropic strains.[60]

DOI: 10.1021/acsbiomaterials.7b00572
ACS Biomater. Sci. Eng. 2018, 4, 502−513

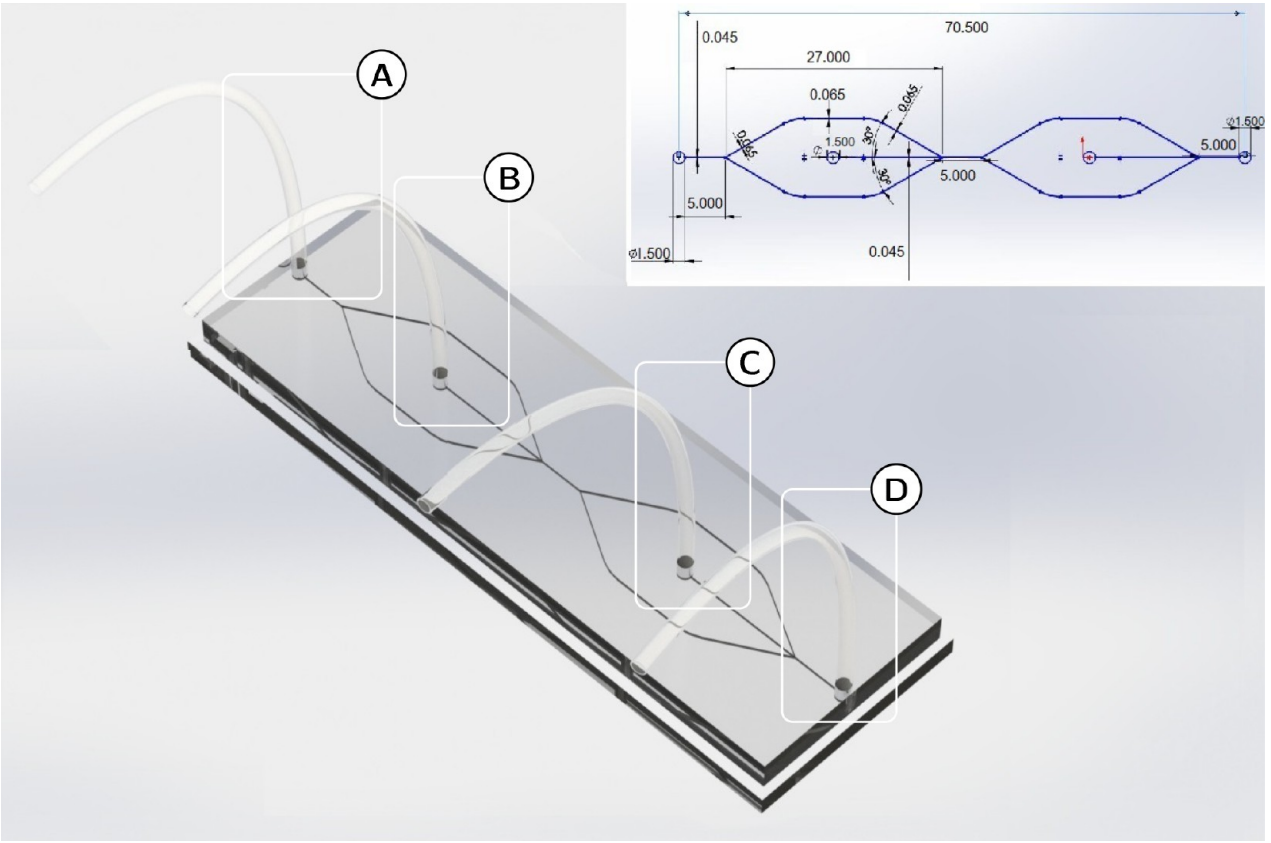

Figure 1. Schematic representation of the different components of the planar 2D flow focusing microfluidic device: (A) Water inlet, (B) lipid/alcohol inlet (DPPC ± DOPG/DDAB in ethanol), (C) loaded molecule for encapsulation (including FITC-LC TAT peptide), and (D) outlet. The upper left inset represents a 2D technical diagram of the design pattern of the device geometry (all dimensions in mm).

MATERIALS AND METHODS

Materials. Negative photoresist (SU-8 2050) was purchased from Microchem Corp. (Boston, MA, USA). Sylgard 184 elastomer kits, consisting of a prepolymer and a curing agent of polydimethylsiloxane (PDMS), were purchased from Dow Corning Corp. (Saint-Laurent, QC, Canada). Tygon 0.020 in. ID microbore tubing was purchased from Cole-Parmer Canada Inc. (Montreal, QC, Canada). A quick setting epoxy adhesive was purchased from LePage-Henkel (Mississauga, ON, Canada). 2-propanol (IPA), acetone and methanol (MeOH), all analytical grade, as well as glass microscope slides were purchased from Fisher Scientific (Waltham, MA, USA). Anhydrous ethyl alcohol (EtOH) was purchased from GreenField Specialty Alcohols Inc. (Brampton, ON, Canada). Trichloro(1H,1H,2H,2H-perfluorooctyl) silane (PFOTS), 1,2-Dioleoyl-*sn*-glycero-3-phosphoglycerol (DOPG) and didodecyldimethylammonium bromide (DDAB) were purchased from Sigma-Aldrich (Oakville, ON, Canada). FITC-LC-TAT fluorescent peptide was purchased from AnaSpec Inc. (Fremont, CA, USA). 1,2-Dipalmitoyl-*sn*-glycero-3-phosphocholine (DPPC) was purchased from Avanti Polar Lipids Inc. (Alabaster, AL, USA). Glass vials were purchased from VWR International (Radnor, PA, USA), 1 and 10 mL Hamilton glass syringes were obtained from Fisher Scientific (Ottawa, ON, Canada). Ultrapure water (Milli-Q) from a Millipore filtration system (resistivity above 18.2 MΩ cm) was used for all experiments.

Methods. *Computer-Assisted Design (CAD).* The design was modeled using a computer aided design (CAD) software (SolidWorks 2016 Dassault S.A., Vélizy, France) and the 2D geometry was exported to be used in computational fluid dynamics (CFD) studies using the "CAD Import Module" in COMSOL. The same design was then used to fabricate the photomask for subsequent microfabrication in the cleanroom.

Numerical Flow Simulations. The microfluidic channel geometry used for simulation (Figure 1) originated from the SolidWorks 2016 sketch used for the experimental fabrication; however, the microfluidic channels leading to and from the flow focusing junction area were truncated to leave only the Y junction of interest. Numerical simulations were then conducted using COMSOL Multiphysics 5.2a (COMSOL Inc., Burlington, MA, USA). The "COMSOL Multiphysics", "CAD Import" as well as the "Microfluidics" Modules were selected. Laminar Flow Models include both 2D "Time-Dependent" and "Steady-State" Analyses. Stationary Steady state studies are governed by "Incompressible Navier-Stokes" and "Continuity" equations where the final forms assuming incompressible Newtonian fluids. A no-slip boundary condition for the walls was applied, to ensure that the modeled fluid comes to rest at the channel walls. Tetrahedral elements were used to mesh the 2D flow-focusing geometry with COMSOL Multiphysics for adaptive mesh refinement. Mesh refinement was manually adjusted around the central flow focusing region and around the edges to get more accurate velocity/concentration profiles. Detailed information regarding the computational parameters and the steady-state equations used for meshing the flow focusing region and representing the flow respectively can be found in the Supporting Information under the CFD section.

Device Manufacturing and Assembly. The microfluidic channels were manufactured via negative photolithography onto a silicon wafer, followed by soft lithography in PDMS. The initial step consists of utilizing the previously constructed CAD geometry to create a chrome photomask. A dark field photomask was obtained from the Center of Microfluidic Systems (CMC, Toronto Ontario, Canada) and used to create a positive mold onto a silicon wafer. The process consists of spinning a negative photoresist, SU-8 2050, at 1700 rpm for 30s to achieve a thickness of 100 μm. Conventional ultraviolet photolithography was performed using the aforementioned photomask, whereby the exposed negative photoresist was cross-linked becoming

DOI: 10.1021/acsbiomaterials.7b00572
ACS Biomater. Sci. Eng. 2018, 4, 502−513

insoluble to the developer. The mold was then treated with PFOTS via chemical vapor deposition to aid with the demolding process. Vacuum is consequently applied, resulting in the vaporization of the silane. After silanizing the master, a PDMS elastomer, was poured onto the previously silanized mold. To prepare the PDMS, an elastomer kit, composed of a prepolymer and a curing agent, was mixed in a 10:1 w/w ratio, as per the manufacturer's protocol. The prepared mixture was poured onto the wafer, which was then degassed in the vacuum desiccator to remove any bubbles within the elastomer and cured at 70 °C for 3 h. Once cured, the channels were carefully cut and removed from the cured polymer with a surgical scalpel or razor blade. A 1.2 mm biopsy punch was then used to puncture the inlet and outlet ports. A representative view of the assembled microfluidic device and its geometry is depicted in Figure 1.

Liposome Fabrication and Loading. The phospholipid-solvent mixtures (DPPC:EtOH) were prepared using DPPC mixed with various ratios of DOPG/DPPG and dissolved directly into EtOH at various concentrations. They were prepared in glass vials (VWR International Radnor, PA, USA) and stored at 4 °C until use. For the encapsulation studies, a 0.5 mg/mL stock solution of fluorescent FITC-LC-TAT peptide was prepared as per the manufacturer's protocol by adding 2 mL of MeOH to a 1 mg of FITC-LC-TAT and stored at 20 °C.

For the bare liposomes fabrication, inlet C was blocked, Milli-Q water flowed through inlet A, and DPPC ± DOPG/DPPG in EtOH flowed through inlet B. For the runs correlating diameter with lipid concentration, DPPC:EtOH solutions at concentrations of 1, 2, 3, 5, and 10 mg/mL were prepared. The flow rate ratios (FRRs), defined as the total volumetric flow rate divided by the focused sheath flow rate, investigated were ranging between 5 and 50. For the peptide encapsulation investigation, the FRR was set to 50 and the DPPC:EtOH concentration was 3 mg/mL. The control batch was prepared by flowing Milli-Q water, 3 mg/mL DPPC:EtOH, and MeOH through inlets A, B, and C, respectively. The same setup was used for encapsulation, with the exception of the incorporation of 0.5 mg/mL FITC-LC-TAT:MeOH flowing through inlet C, i.e., loaded. Detailed batch descriptions can be found in the Supporting Information.

Characterization. *Zeta Potential Measurements.* ITo quantify their colloidal stability, the zeta potential of the liposomes was measured using a Zetasizer Nano ZS (Malvern, UK). The samples were analyzed for ten cycles with a voltage of 4 mV.

Size/Concentration Measurements. To evaluate the size of the loaded and unloaded liposomes (both prior and following FITC-LC-TAT peptide encapsulation), dynamic light scattering (DLS) measurements were compared with nanoparticle tracking analysis (NTA) measurements in order to characterize the particles size, size distribution, polydispersity index (PDI), and concentration.

Dynamic Light Scattering (DLS). The particle diameters were determined by use of dynamic light scattering (DLS) via a ZetaPALS Zeta Potential Analyzer (Brookhaven Instruments Corp., Holtsville, NY, USA). DLS relies on the Brownian motion of particles suspended in a solution to obtain a diffusion coefficient, from which the particle size is determined. A red laser (675 nm) is emitted at a 90° angle, with the recording chamber temperature set to 26 °C. Each run consisted of ten 10 s readings.

Nanoparticle Tracking Analysis (NTA). NTA was also used for detecting simultaneously submicron particle size distributions and particle concentrations of multiples samples. Measurements were performed with a NanoSight LM14 (NanoSight, Amesbury, United Kingdom), equipped with a sample chamber with a 640 nm laser and a Viton fluoro-elastomer O-ring. The samples were injected in the sample chamber with sterile syringes (BD Discardit II, New Jersey, USA) until the liquid reached the tip of the nozzle. The samples were measured for 40 s with manual shutter and gain adjustments. All measurements were performed at room temperature (T = 25 °C). Data was processed by the NTA 3.2 Build 127 software.

Imaging and Visualization. Negative Staining. Samples for negative staining were prepared using the Single-droplet method.[61] After preparing a 2% aqueous solution of an uranyl acetate stain (and adjusting the pH to 7.0 with 1 M KOH when required), Formvar-carbon coated grids were glow discharged in order to increase their hydrophilicity prior to their use. A volume of 5 μL was then pipetted on the grid so as to cover the entirety of the grid surface. After approximately 10 s, 5 μL of the uranyl acetate stain was slowly pipetted onto the sample, and the stain absorbed from the opposite side using a wedge of filter paper. The grid was then allowed to dry and then examined by TEM (transmission electron microscopy). Samples were imaged at a magnification of 50 000× at room temperature using a Philips Tecnai T12 electron microscope equipped with an LaB6 filament and operated at an acceleration voltage of 120 kV.

Device Flow Visualization. The fluid flow rates were controlled with a Nexus 3000 syringe pump (Chemyx Inc., Stafford, TX, USA) in conjunction with syringes of various volumes (BD Medical, Mississauga, ON, Canada). The image acquisition setup consisted of an inverted microscope (Eclipse TE 2000-U, Nikon Corp, Mississauga, ON, Canada), with fluorescence capabilities, which was used to visualize the liposomes as well as the fluorescence emission from the FITC-LC-TAT peptide. All images were captured using a CCD camera (Retiga-2000R, Q imaging, Surrey, BC, Canada) and Nikon NIS-Elements D software. Milli-Q water, colored with readily available food dyes, was used as the working fluid. The pumps were set to flow at various flow rates and images of the flow focusing junctions were obtained at low (20×) and high (40×) magnifications.

Particle Count. An open-source software; CellProfiler, was used to quantitatively measure the fluorescent particles count. A pipeline was custom developed for detection of drug encapsulating liposomes. The pipeline has four major steps: (1) background correction, (2) colony detection & filtering, (3) measuring colony parameters, and (4) overlaying images. Background correction was done through its own inherent modules, Color to Gray, Correct Illumination calculation, and Correct Illumination Apply modules for object detection (Identify Primary Objects) were based on thresholding and are available in Cell Profiler.

Statistical Analysis. Data are expressed as mean ± standard error (SE) or standard deviation (SD) of five replicates or more per group. Statistical analyses were performed for multiple comparisons via one-way ANOVA and Student's t test was used for direct result comparison. Differences were considered significant at $p < 0.05$.

RESULTS AND DISCUSSION

To fully characterize the HFF device and its liposomes synthesis and loading capabilities, we first conducted flow visualization of the flow focusing junction to qualitatively visualize the effect of varying the FRR on the width and behavior of the focused stream at the focusing junction. A comparison between the simulated flows, computed using Comsol Microfluidics and the experimental flows inside the platform as imaged by optical microscopy is therefore provided. Next, visualization of the synthesized liposomes was conducted by negative stating TEM microscopy thus offering both a quantitative and qualitative representation of the shape and morphology as well as the size of synthesized liposomes in aqueous conditions. Finally, the effect of varying both the lipid composition and flow parameters for the synthesis of DPPC nanosized liposomes within the platform was assessed with regards to size, concentration, charge, and polydispersity of the resulting nanoliposomes.

Comparison between Experimental and Simulated Flows. Initial attempts at hydrodynamic focusing were aimed at confining sample flow to a narrow, planar column, which is now commonly referred to as two 2D flow focusing.[62] The possibility of significant microfluidic focusing in 2D was first demonstrated by confining a sample flow from a 10 μm nozzle to a width of only 50 nm.[63]

Liposomes formation in HFF occurs under laminar fluid flow conditions and is driven by a diffusively driven process

DOI: 10.1021/acsbiomaterials.7b00572
ACS Biomater. Sci. Eng. 2018, 4, 502−513

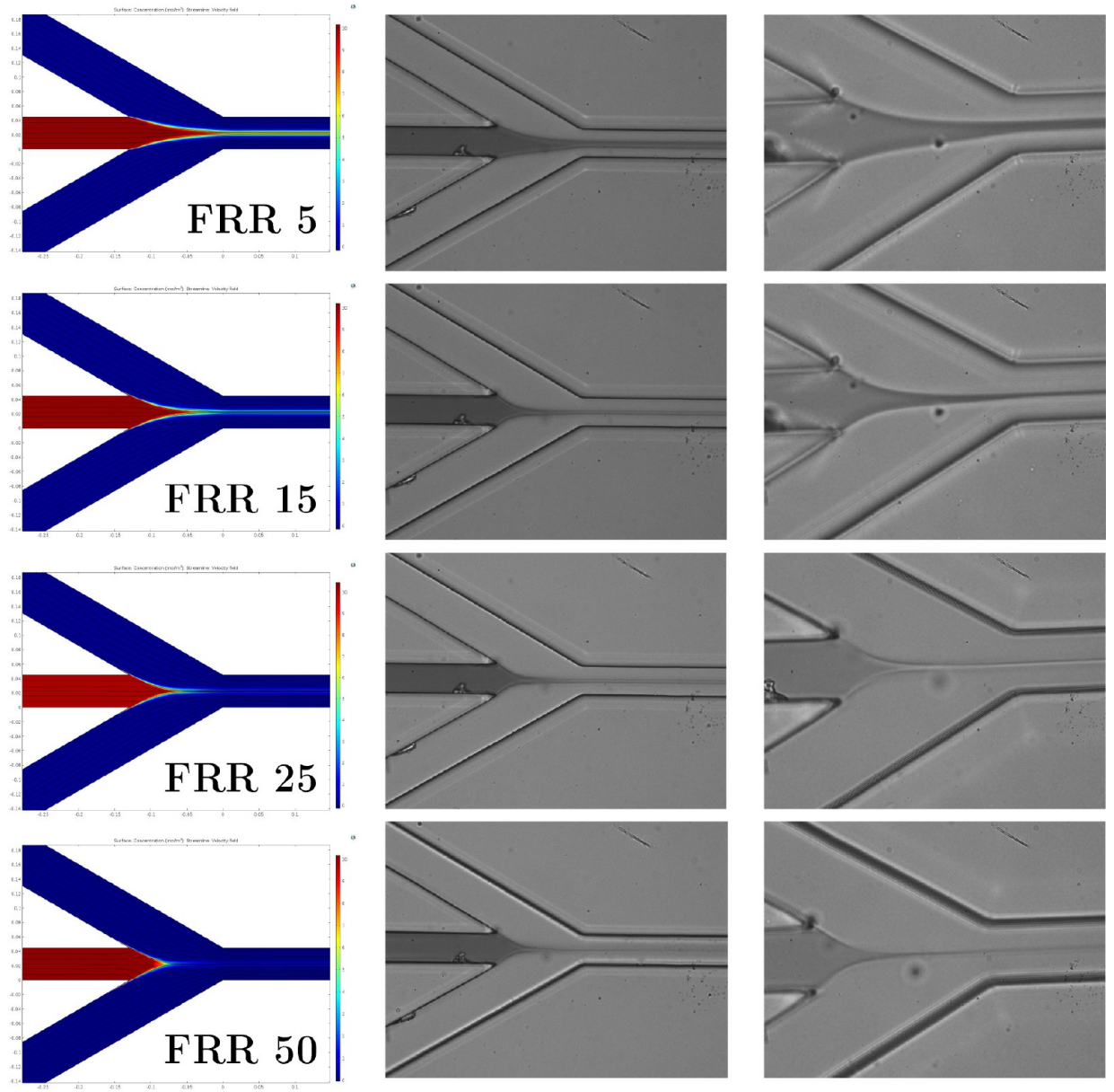

Figure 2. Comparison between 2-dimensional model simulations of the concentration profile at the focusing junction for the respective FRRs of 5 (Re = 0.6), 15 (Re = 7.0), 25 (Re = 21.2) and 50 (Re = 74.3) and the focused stream imaged with an optical microscope at 20× and 40×, respectively.

influenced by convection at higher FRRs.[45] Lower FRRs result in a relatively wide center stream in which mixing time is limited by molecular diffusion in a direction which is normal to the streamlines.[45] This leads to a relatively shallow concentration gradient, a lower surface-to volume ratio, and a gradual depletion of the focused center stream by mutual diffusion of the two fluids across the contact interface. As a result, a large fraction of lipid molecules remains solubilized and self-assembles into larger liposomes (as measured experimentally by DLS and NTA) in the downstream diffusive mixing channel, whereas the fraction of liposomes that forms in the convective−diffusive focusing region is low. Conversely, high focusing, that is, FRR 15−50 result in a narrower center stream in which mixing time becomes dominated by two-dimensional convective−diffusive transport in the focusing region.[45] Convection abruptly reduces the width of the focused stream in the hydrodynamic focusing region, which reduces the diffusion length, enhances diffusive mixing, and results in a steep concentration gradient. High focusing results in a relatively high surface-to-volume ratio and the rapid depletion of the focused center stream by convective-diffusive mixing, causing more of the lipid molecules to self-assemble into smaller liposomes (as measured experimentally by DLS and NTA). Further increases in FRR gradually change this mixing condition until a minimum mixing time is reached.[45] Light microscopy images of the focusing stream at magnifications of (20×) and (40×) are shown for different flow rate ratios (FRRs) in Figure 2, which depicts the focusing of a central lipid stream (dark stream) by two aqueous water streams (not visible). The main concept of HFF is to reduce the stream width and consequently the mixing path length of the focused stream. A stream of lipids resolubilized in ethanol is hydrodynamically focused into a very narrow sheet with a thickness varying from a few micrometers down to submicrometers depending on the respective water-to-ethanol volumetric flow rate ratios (FRRs).[64] The focused stream at the center of the flow

DOI: 10.1021/acsbiomaterials.7b00572
ACS Biomater. Sci. Eng. 2018, 4, 502−513

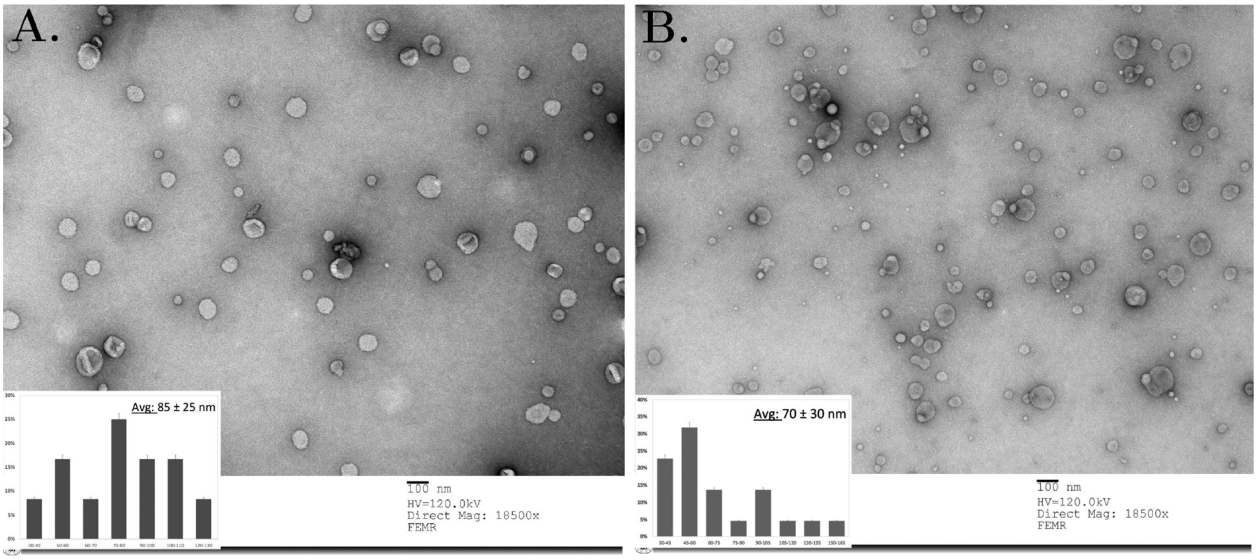

Figure 3. Transmission electron microscopy (TEM) image of the DPPC:EtOH liposomes after negative staining at FRR = 30 for: (A) C = 5 mg/mL, and (B) C = 10 mg/mL. The small insets show the size distribution of the particles as measured by Cell Profiler with the average value (in nm ± SD).

focusing junction is not always centered along the midline of the channel or symmetrical as shown in Figure 2. For low Reynolds numbers (Re < 5), a slightly convex shape of the focused streams is generated and is to be expected in microfluidic channels due to viscous forces dominating inertial ones.[65] This can cause flow disturbances in a way reminiscent of that of a turbulent flow at high Re numbers.[66] This phenomenon can be observed in this flow focusing device at low FRRs (such as FRR 5), where it is observed that the flow is asymmetrical with a tendency to lean toward the upper side of the central channel wall. Retrospectively, a higher polydispersity and SD of the particles diameters at low FRRs compared to high FRRs is therefore expected, where a better control of the flow focusing enables a constant more laminar flow.

Flow-focusing was first examined from the plan view (Figure 2), to compare the focused alcohol stream in a the 65 μm wide central microchannel and the two 45 μm wide side microchannels, imaged with an optical microscope and the 2D model simulation for the respective FRRs of 5, 10, 20, and 50 for flow rates corresponding to 40, 90, 190, and 490 μL/min. Overall, the 2D simulation results were well-substantiated with the experimental findings. The shape and width of the focused ethanol stream was well represented in the simulation with a tendency to decrease its thickness with an increase in the FRR. Experimental investigations indicated that in the case of symmetric side streams focused flow sheet was not necessarily uniform with undesirable thickening close to the walls of a microchannel observed in the case of low FRRs (Figure 2). By manipulating flow rates of the focusing flows, location of the focused sheet could be deformed and moved out of the symmetry plane and most importantly, a precise control of the width of the focused stream, on which the size and polydispersity of the generated liposomes depend on, was achieved. Maintaining a precise control of the focused stream width is crucial in various applications of the flow focusing systems.[67]

Visualization of Liposomes by Negative Staining Electron Microscopy. Figure 3 shows the DPPC:EtOH liposomes formed at a flow rate ratio of FRR = 30 and a concentration of C_{DPPC} = 10 mg/mL and C_{DPPC} = 5 mg/mL respectively.

At the former condition (FRR = 30, C_{DPPC} = 10 mg/mL), the liposomes particles are spherical and mostly unilamellar. Although no clear correlation between the concentration of DPPC and the size of the liposomes could be drawn from TEM images alone, regardless, at high sample concentrations (C_{DPPC} = 10 mg/mL; Figure 3A), liposomal population appear bigger in size, with fewer particles below 30 nm observed than at C_{DPPC} = 5 mg/mL (Figure 3B). In some cases, the shape of liposomes appeared distorted. This could be attributed to both the HFF process and to the negative staining technique as well.[68] Although the electronic microscopy technique ensures the complete structural analysis of the thin transparent samples,[69] possible artifacts could be due both to the staining process (the interaction between the sample and the negative stain) and the distortion/alteration induced during the drying steps caused by the exposition of the samples to a vacuum.[61] In fact, as part of the drying processes, the particle loses its hydration shell. Often, this shell stabilizes the soluble particle onto a certain configuration and deposition on the carbon can cause it to change shape.[61]

Effect of Experimental Parameters on Liposome Size and Size Distribution. The size distribution of lipid particle with respect to the FRR between the lipid and water streams has been measured by DLS and plotted for every concentration. Different DPPC concentrations in ethanol have been tested namely (C_{DPPC} = 1, 2, 3, 5, and 10 mg/mL). Figure 4A shows all the graphs combined and displays the complete size distribution profile for all the lipid concentration of DPPC in ethanol for concentration ranging from 1 to 10 mg/mL. A logarithmic tendency curve has been fit to all the concentration profiles.

Different microfluidic techniques have been shown to produce uniformly dispersed liposomes and allow for direct control of liposome size via fine adjustments to the FRR. Decreasing the sample stream width to micrometer length scales allows for controlled and reproducible mechanical and chemical conditions across the stream width, especially

DOI: 10.1021/acsbiomaterials.7b00572
ACS Biomater. Sci. Eng. 2018, 4, 502−513

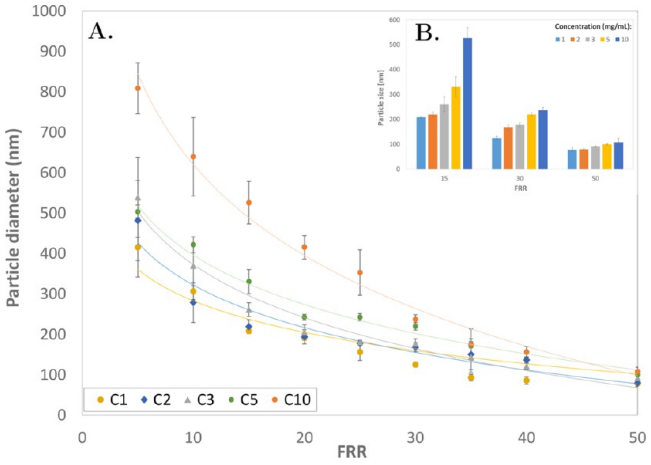

Figure 4. (A) Particle size distribution profiles of 2D HFF synthesized liposomes as a function of DPPC lipid concentration at inlet (C = 1−10 mg/mL) for various FRRs (5−50), with (B) a stacked histogram representation of the NPs size distribution at given concentrations (C = 1−10 mg/mL) and FRRs (15, 30, and 50) ($n \geq 15$).

compared to more traditional bulk-phase preparation techniques (i.e., test tubes and beakers).[25] It has been found that the mean diameter of the liposomes produced to be directly related to lipid concentration and inversely related to the FRR.[25,26] In contrast, the effect of the total flow rate (TFR) on liposome size in more controversial. Previous reports have suggested that the vesicle size distribution remains nearly unaffected by the total volumetric flow rate (TFR).[50,70] Other sources claim that although it has little impact on the average vesicle size at high focusing conditions, its effect on the liposome diameter increased noticeably toward low focusing conditions.[45] Both lipid and ethanol concentration have been proven to have a significant effect on liposome properties (in both bulk and microfluidic methods).[50] The mean diameter of the liposomes produced is directly related to lipid concentration.[36]

From Figure 4A, B, we observe that at high DPPC lipid concentration (10 mg/mL) and low flow rate ratios (FRRs ≈ 5−10), particle sizes reach almost a micron (650−850 nm). However, at high FRR = 50, the particle size is significantly smaller, in the range of 100 nm for almost every concentration (C_{DPPC} = 1−10 mg/mL). At low concentration, the flow and particle formation is less predictable and stable respectively so the standard error is bigger. A better illustration of the effect of FRR on the sizes of the colloidal liposomal dispersions as a function of DPPC concentrations is presented in Figure 4B. A distinct tendency of an increase of particle size with both a decrease in FRR and an increase in DPPC concentration is recorded. In addition, as the flow rate ratio (FRR) increases from 15 to 50, the differences in particle sizes at various concentrations are significantly smaller. For example, the size was almost doubled (550 nm in average) at FRR = 15 and C_{DPPC} = 10 mg/mL than at FRR = 15 and C_{DPPC} = 5 mg/mL where they average ∼350 nm. In addition, all liposomal DPPC formulations exhibited homogeneity with a polydispersity index (PDI) of less than 0.35. Overall, the average PDI index (an estimate of the width of the distribution) was higher at a lower FRRs and for lower DPPC concentrations. Average values of the polydispersity index for the liposomes prepared at two different FRRs (15 and 50) as various DPPC concentrations (in mg/mL) are reported in the Supporting Information.

After confirming the core−shell structure of the lipid NPs, and knowing their range of size distribution based on the change in FRR, we investigated the possibility of controlling the NP's physicochemical properties, mainly size and surface charge while keeping other conditions such as lipidic and aqueous flow rates and flow ratios. Both the zeta potential (ZP) of colloidal systems and their size exert a major effect on the various properties of nanodrug delivery systems. Not only the stability of dosage forms and their release rate are affected but also their circulation in the bloodstream and absorption into body membranes are dramatically altered by the ZP.[71] The coating material studied is often limited to neutral or anionic lipid mixtures such as DMPC or DPPC. Limited data are provided on the comparison between different lipid mixtures or on the use of cationic lipids, which may be more suitable for medical or biotechnological applications (e.g., as delivery systems for anticancer drugs or as transfection reagents), and which are routinely used in the industry.[50] Using DPPC as the main bilayer constituent, the effect of adding negatively charged DOPG or positively charged DDAB lipid molecules at different weight ratios to the lipid stream on the resulting liposome diameters and charge is investigated. The composition of the

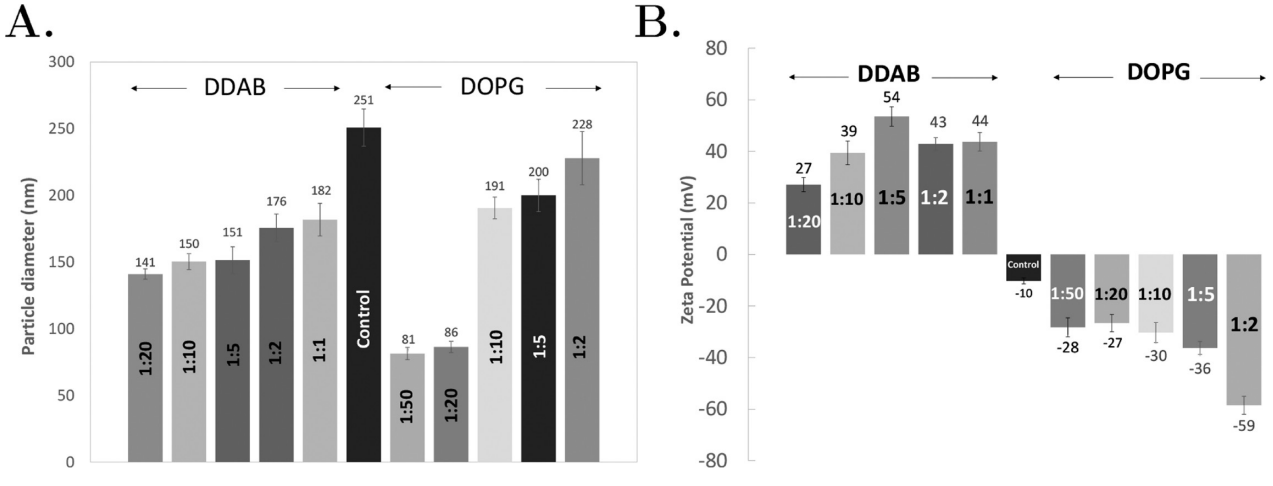

Figure 5. (A) Particle size distribution and (B) zeta potential measurements of synthesized DPPC liposomes with different DOPG/DDAB weight ratios ($n \geq 10$).

DOI: 10.1021/acsbiomaterials.7b00572
ACS Biomater. Sci. Eng. 2018, 4, 502−513

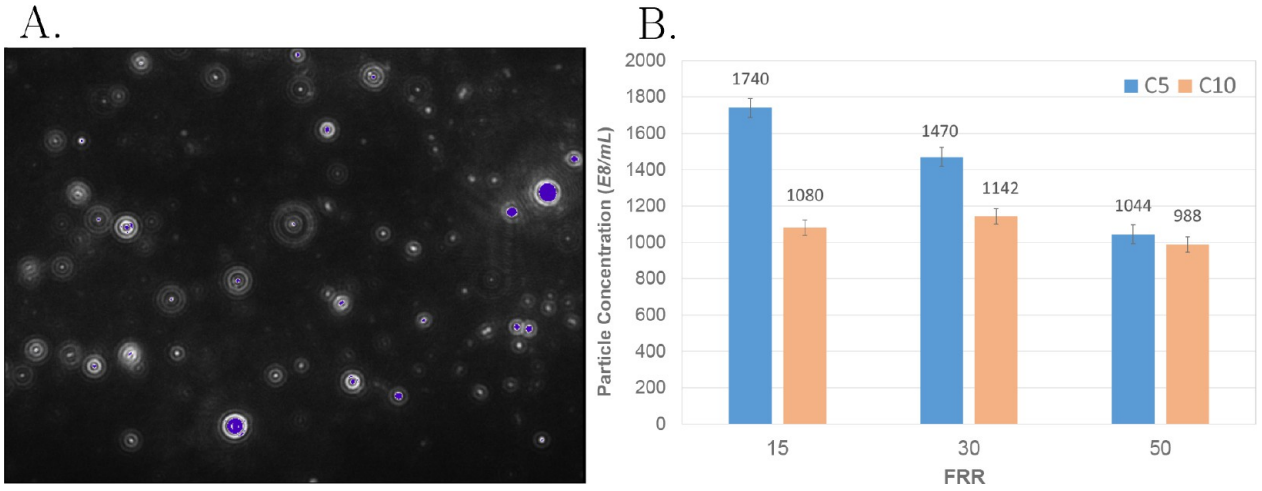

Figure 6. (A) NTA video frame showing diluted liposomes particles at C_{DPPC} = 5 mg/mL, FRR= 30 (dilution = 100). Measured size by NTA = 250 ± 50 nm (see Video S1). (B) Particle concentration (× 10^8 particles/mL) of the synthesized liposomes as a function of DPPC concentration (mg/mL) and FRR. The error bars displayed on the NTA graphs were obtained by the standard error of the different measurements of each sample ($n \geq 10$).

batch samples can be found in the Supporting Information under the Liposome Synthesis section.

As shown in Figure 5B, whereas the control (C_{DPPC} = 5 mg/mL) has a low −10 mV zeta potential, adding DDAB and DOPG either positively or negatively increases the charge. In fact, adding DDAB at a 1:5 ratio to the control C_{DPPC} = 5 mg/mL solution yields a high zeta potential of approximately 50 mV and results in highly stable lipid particles. On the other hand, adding DOPG gives a highly negative charge to the DPPC: EtOH particles with the maximum being at −30 for a 1:10 ratio, which corresponds to a good particle stability. Further studies at higher DOPG: DPPC ratio need to be tested and a compromise between charge and size need to be found as this ratio (1:10 DOPG:DDPC gives the biggest size particles approximately 191 nm).

For DOPG, high weight ratio gives solutions that are less homogeneous. For both conditions, a weight ratio of 1:5 constitutes the best compromise between size/stability.

Overall, results showed that the surface charge and size of the microfluidic synthesized liposomes can be finely tuned by changing the lipid stream composition and incorporating molecules with positively or negatively charged functional groups. Charge modification of nanosystems offers an opportunity for prolonging the blood circulation time of drugs, enhancing the possibility of its interaction with target cells of interest, and changing the pharmaceutical properties of nanosystems.[3]

Effect of DPPC Concentration on Yield and Size Distribution of Liposomes. Nanoparticle tracking analysis (NTA) was used for the analysis of diluted samples of nanosized lipid particles and liposomes aggregates. A direct comparison with DLS was made in order to gain a more complete estimation of the size distribution of liposomes at various conditions. Figure 6 shows the HFF synthesized liposomal particles (C_{DPPC} = 5 mg/mL, FRR = 30) visualized by NTA.

Using the NTA technique, particles are seen as point scatterers moving under Brownian motion, with larger particles scattering significantly more light and appearing bigger.[72] The high resolution of the NTA make it possible to get an estimation of the sample polydispersity at any given condition (concentration, FRR) before quantitative capture and measurement. In Figure 6a, the sample captured is fairly monodispersed, with a polydispersity similar to what was observed by negative TEM microscopy.

Figure 6 displays the NTA particle concentration measurements at two different concentrations (C_{DPPC} = 5 and 10 mg/mL) and for three different flow rate ratios (FRR = 15, 30 and 50). An inverse correlation between concentrations of lipid DPPC in ethanol and liposome particle concentration can be observed with DPPC solutions at C = 5 mg/mL being 37.9% more concentrated than solutions at C= 5 mg/mL at a FRR = 15 and more than 22.3% at FRR = 30. At FRR = 50, however, no significant difference of concentration is noted between the two different DPPC concentrations (C = 5−10 mg/mL). Alternatively, for a constant concentration of C_{DPPC} = 10 mg/mL, the difference in liposomal concentration is not significant at the various FRRs. On the other hand, for C_{DPPC} = 5 mg/mL, a tendency of a decrease in sample concentration with an increase in FRR can be observed. This difference amounts to more than 15.5% between FRR15−30 and to ∼29.0% between FRR 30−50. Hydrodynamic flow-focusing technique using planar microfluidic devices for liposome formation is characterized as a low-throughput process because of the limited volumetric flow rates imposed by the small channel dimensions generally used although so far, no quantitative estimate of the concentration of the produced particles has been cited. The maximum flow rate and phospholipids concentration are generally restricted by limitations associated with fluid rheological behavior, which can increase internal pressurem leading to clogging issues.[51] Overall, it is concluded that both DPPC concentration and FRR have a significant impact on the concentration of liposomes obtained by HFF synthesis, with the FRR playing a bigger influence on the resulting particle concentration to that played by the inlet concentration of DPPC.[43] Live monitoring and sample visualization as well as individual particle tracking are features that enabled a thorough size distribution analysis and made possible the characterization of the synthesized liposomal NPs, complementing DLS.

DOI: 10.1021/acsbiomaterials.7b00572
ACS Biomater. Sci. Eng. 2018, 4, 502−513

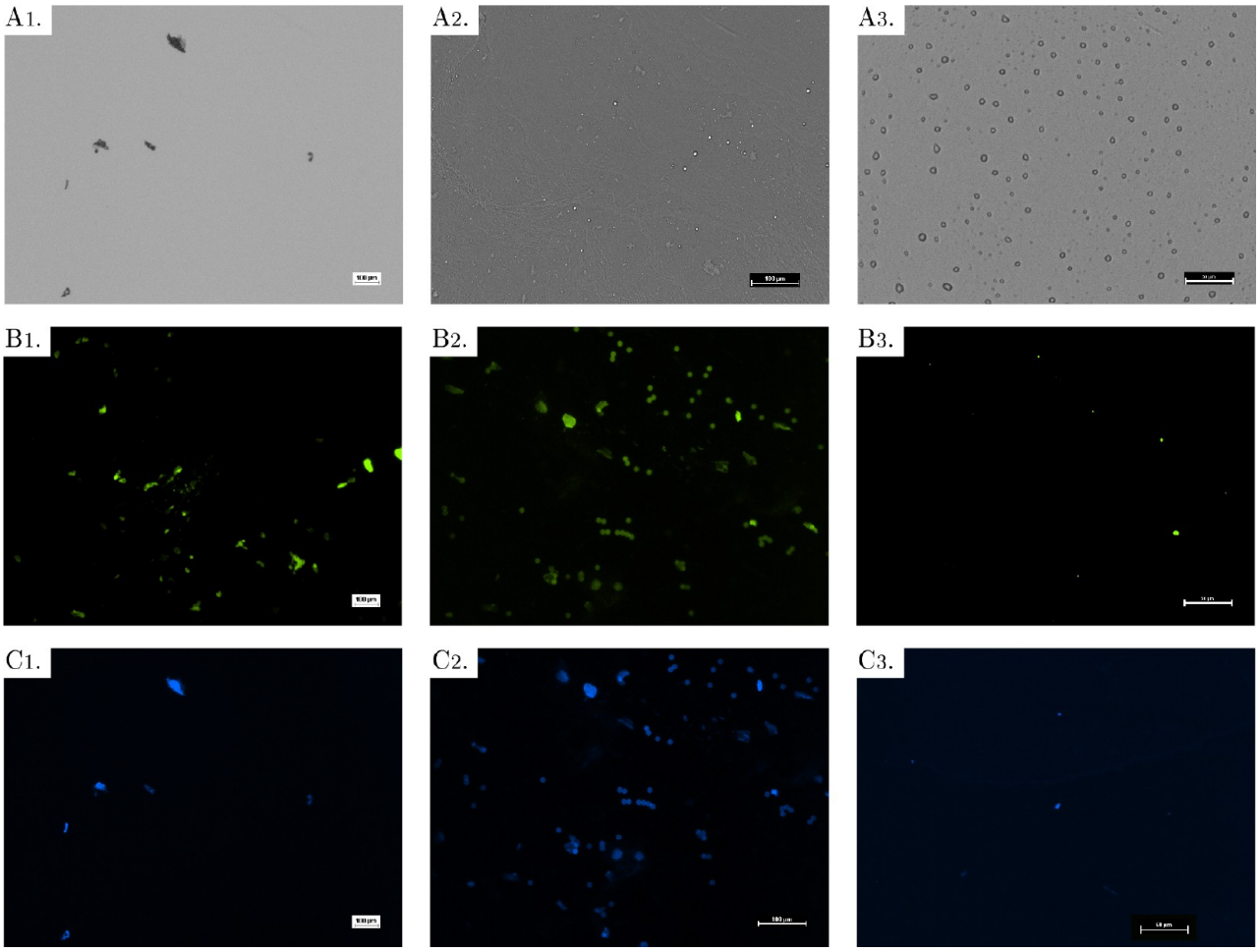

Figure 7. Optical imaging of a liposomes encapsulating FITC (fluorescein isothiocyanate)-labeled LC-TAT peptide using different filters: FITC green (B1, B2, and B3) and DAPI blue (C1, C2, and C3) at 10×(A1, B1, and C1), 20× (A2, B2, and C2), and 40× (A3, B3, and C3).

■ ENCAPSULATION OF FITC-LC TAT

Subsequently, liposomes containing FITC-LC TAT were observed via microscopy. The representative sets of figures (Figure 7) are visualized under fluorescence with the FITC filter, DAPI, and light microscopy of on-chip, passively loaded FITC-LC TAT nanoliposomes.

After setting the DPPC concentration and FRR for liposomal synthesis to 3 mg/mL and 30, respectively, FITC-LC-TAT encapsulation was attempted. Approximately 1 mL of product was obtained in less than three and a half minutes, with larger volumetric outputs, and in turn faster production times, achievable simply by increasing the fluid flow rates. As an example, by increasing the FRR to 50, 1 mL of liposomes encapsulating molecules can be made in approximately 2 min. Detailed preparation times for every FRR can be found in the Supporting Information. From Figure 7, it can be observed that the fluorescence and vesicles overlap. Liposomes should not be affected by the loading time due to the minute volume of solvent present in the mixture.[43] The fluorescence images in Figure 7 imply that the FITC-labeled LC-TAT peptide was successfully encapsulated within the liposomes. Optical microscopy (not shown here) comparing batches of encapsulated liposomes with the fluorescent peptide prior and following filtration by dialysis confirmed the absence of any free FITC-LC-TAT peptides. A quantitative estimate of the number of encapsulated FITC-LC-TAT peptide in liposomes is provided in the Supporting Information that shows the automated particle count averaged over the microscopy areas (B1−B3, C1−C3) in Figure 7.

From the encapsulation results, the microfluidic platform is therefore demonstrated to control liposome formation and compound encapsulation in a way that compete with existing conventional methods in liposome size homogeneity and adjustable encapsulation. Confining a water-soluble compound to be encapsulated to the immediate vicinity where liposome formation occurs has the added advantage of reducing sample consumption without affecting liposome loading.[25] Moreover, having a precise control over the concentration and amount of encapsulated compounds within liposomes in a continuous-flow mode is another interesting feature of this platform.

■ CONCLUSION

In the present study, we have demonstrated the use of a microfluidic flow-focusing device for the continuous synthesis and loading of DPPC liposomes. This simple, low-cost, and easily scalable in parallel double flow-focusing device, enabled reproducible control of the size and size distribution of nanosized liposomal particles. With this platform, we reduced both the number of different apparatus required for liposomal fabrication as well as the amount of steps needed for the synthesis of monodisperse liposomes. Results revealed an interesting trend where increasing the dissolved phospholipid

DOI: 10.1021/acsbiomaterials.7b00572
ACS Biomater. Sci. Eng. 2018, 4, 502−513

concentration resulted in an increase in the particle diameter. Additionally, we established a correlation between increasing the FRR and the resulting decrease in particle diameter with a plateau reached around 60 nm. The ability to alter the concentration and control the amount of encapsulated compounds within liposomes in a continuous-flow mode is another interesting feature toward tailored liposomal drug delivery for cancer therapy.[26] Future work should focus on the quantitative evaluation of the encapsulation efficiency of the loaded liposomes. This can be achieved via application specialized tools such as fluorescence fluctuation analysis (FFA) and multiangle laser light scattering (MALLS) in conjunction with asymmetric field flow fractionation (AFFF) to measure the entrapment efficiency of the loaded liposomes.[45] Overall, these findings suggest that this platform would provide the possibility of the development and optimization of not only liposomes but also various nano/microparticulate systems in the emerging field of nanomedicine, along with offering the possibility of loading multiple encapsulated agents during their synthesis in a very time-effective manner. Such a microfluidic platform can control their self-assembly and potentially lead to applications as part of point-of-care personalized therapeutics. However, the problem of scaling up the nano/microparticulate systems production needs to be addressed during the implementation of microfluidics technology for practical applications.[44]

■ ASSOCIATED CONTENT

Supporting Information

The Supporting Information is available free of charge on the ACS Publications website at DOI: 10.1021/acsbiomaterials.7b00572.

CFD parameters and simulations, liposome synthesis protocols, NTA reports and video captures (PDF)
Video S1 (ZIP)
Video S2 (ZIP)

■ AUTHOR INFORMATION

Corresponding Author

*E-mail: maryam.tabrizian@mcgill.ca. Phone: +1 514-398-8129. Fax: +1 514-398-7461.

ORCID

Maryam Tabrizian: 0000-0002-5050-4480

Notes

The authors declare no competing financial interest.

■ ACKNOWLEDGMENTS

The authors extend their gratitude to the National Science and Engineering Research Council of Canada (NSERC) for their financial support towards this research. The authors also acknowledge the CGS-Masters Scholarship awarded to S.A. as well as the NSERC-CREATE grant in Continuous Flow and the Discovery grant awarded to M.T.

■ REFERENCES

(1) Mozafari, M. R; Johnson, C.; Hatziantoniou, S.; Demetzos, C. Nanoliposomes and Their Applications in Food Nanotechnology. *J. Liposome Res.* **2008**, *18*, 309−327.

(2) Lin, C.-M.; Li, C.-S.; Sheng, Y.-J.; Wu, D. T.; Tsao, H.-W. Size-Dependent Properties of Small Unilamellar Vesicles Formed by Model Lipids. *Langmuir* **2012**, *28*, 689−700.

(3) Blanco, E.; Shen, H.; Ferrari, M. Principles of nanoparticle design for overcoming biological barriers to drug delivery. *Nat. Biotechnol.* **2015**, *33*, 941−951.

(4) Bowey, K.; Tanguay, J.-F.; Tabrizian, M. Liposome technology for cardiovascular disease treatment and diagnosis. *Expert Opin. Drug Delivery* **2012**, *9*, 249−265.

(5) Akbarzadeh, A.; Rezaei-Sadabady, R.; Davaran, S.; Joo, S. W.; Zarghami, N.; Hanifehpour, Y.; Samiei, M.; Kouhi, M.; Nejati-Koshki, K. Liposome: classification, preparation, and applications. *Nanoscale Res. Lett.* **2013**, *8*, 102.

(6) Brandl, M. Liposomes as drug carriers: a technological approach. *Biotechnol. Annu. Rev.* **2001**, *7*, 59−85.

(7) Chattopadhyay, P.; Shekunov, B.; Yim, D.; Cipolla, D.; Boyd, B.; Farr, S. Production of solid lipid nanoparticle suspensions using supercritical fluid extraction of emulsions (SFEE) for pulmonary delivery using the AERx system? *Adv. Drug Delivery Rev.* **2007**, *59*, 444−453.

(8) Walde, P. Preparation of Vesicles (Liposomes). In *Encyclopedia of Nanoscience and Nanotechnology*; American Scientific Publishers: Stevenson Ranch, CA, 2004; Vol. 9, pp 43−79.

(9) Sankar Kadimi, U.; Balasubramanian, D. R.; Ganni, U. R.; Balaraman, M.; Govindarajulu, V. In vitro studies on liposomal amphotericin B obtained by supercritical carbon dioxide mediated process. *Nanomedicine* **2007**, *3*, 273−280.

(10) Conchouso, D.; Castro, D.; Khan, S. A.; Foulds, I. G. Three-dimensional parallelization of microfluidic droplet generators for a litre per hour volume production of single emulsions. *Lab Chip* **2014**, *14*, 3011.

(11) Kunastitchai, S.; Pichert, L.; Sarisuta, N.; Muller, B. W. Application of aerosol solvent extraction system (ASES) process for preparation of liposomes in a dry and reconstitutable form. *Int. J. Pharm.* **2006**, *316*, 93−101.

(12) Cano-Sarabia, M.; Ventosa, N.; Sala, S.; Patino, C.; Arranz, R.; Veciana, J. Preparation of Uniform Rich Cholesterol Unilamellar Nanovesicles Using CO2-Expanded Solvents. *Langmuir* **2008**, *24*, 2433−2437.

(13) Ong, S.; Ming, L.; Lee, K.; Yuen, K. Influence of the Encapsulation Efficiency and Size of Liposome on the Oral Bioavailability of Griseofulvin-Loaded Liposomes. *Pharmaceutics* **2016**, *8*, 25.

(14) Shariat, S.; Badiee, A.; Jalali, S. A.; Mansourian, M.; Yazdani, M.; Mortazavi, S. A.; Jaafari, M. R. P5 HER2/neu-derived peptide conjugated to liposomes containing MPL adjuvant as an effective prophylactic vaccine formulation for breast cancer. *Cancer Lett.* **2014**, *355*, 54−60.

(15) Costa, A. P.; Xu, X.; Burgess, D. J. Freeze-Anneal-Thaw Cycling of Unilamellar Liposomes: Effect on Encapsulation Efficiency. *Pharm. Res.* **2014**, *31*, 97−103.

(16) Pattni, B. S.; Chupin, V. V.; Torchilin, V. P. New Developments in Liposomal Drug Delivery. *Chem. Rev.* **2015**, *115*, 10938−10966.

(17) Batzri, S.; Korn, E. D. Single bilayer liposomes prepared without sonication. *Biochim. Biophys. Acta, Biomembr.* **1973**, *298*, 1015−1019.

(18) Lohse, B.; Bolinger, P.-Y.; Stamou, D. Encapsulation Efficiency Measured on Single Small Unilamellar Vesicles. *J. Am. Chem. Soc.* **2008**, *130*, 14372−14373.

(19) Olea, D.; Faure, C. Quantitative study of the encapsulation of glucose oxidase into multilamellar vesicles and its effect on enzyme activity. *J. Chem. Phys.* **2003**, *119*, 6111.

(20) Kerdudo, A.; Dingas, A.; Fernandez, X.; Faure, C. Encapsulation of rutin and naringenin in multilamellar vesicles for optimum antioxidant activity. *Food Chem.* **2014**, *159*, 12−19.

(21) Valencia, P. M.; Farokhzad, O. C.; Karnik, R.; Langer, R. Microfluidic technologies for accelerating the clinical translation of nanoparticles. *Nat. Nanotechnol.* **2012**, *7*, 623−629.

(22) Meure, L. A.; Foster, N. R.; Dehghani, F. Conventional and Dense Gas Techniques for the Production of Liposomes: A Review. *AAPS PharmSciTech* **2008**, *9*, 798.

DOI: 10.1021/acsbiomaterials.7b00572
ACS Biomater. Sci. Eng. 2018, 4, 502−513

(23) Allen, T. M.; Cullis, P. R. Liposomal drug delivery systems: From concept to clinical applications. *Adv. Drug Delivery Rev.* **2013**, *65*, 36−48.
(24) Al-Jamal, W. T.; Kostarelos, K. Liposomes: From a Clinically Established Drug Delivery System to a Nanoparticle Platform for Theranostic Nanomedicine. *Acc. Chem. Res.* **2011**, *44*, 1094−1104.
(25) Jahn, A.; Vreeland, W. N.; Gaitan, M.; Locascio, L. E. Controlled Vesicle Self-Assembly in Microfluidic Channels with Hydrodynamic Focusing. *J. Am. Chem. Soc.* **2004**, *126*, 2674−2675.
(26) Jahn, A.; Vreeland, W. N.; DeVoe, D. L.; Locascio, L. E.; Gaitan, M. Microfluidic Directed Formation of Liposomes of Controlled Size. *Langmuir* **2007**, *23*, 6289−6293.
(27) Zhang, H. *Liposomes: Methods and Protocols*; Springer: New York, 2017; pp 17−2210.1007/978-1-4939-6591-5.
(28) Valle, M. J.; Navarro, A. Liposomes Prepared in Absence of Organic Solvents: Sonication Versus Lipid Film Hydration Method. *Curr. Pharm. Anal.* **2015**, *11*, 86−91.
(29) Varona, S.; Martin, A.; Cocero, M. J. Liposomal Incorporation of Lavandin Essential Oil by a Thin-Film Hydration Method and by Particles from Gas-Saturated Solutions. *Ind. Eng. Chem. Res.* **2011**, *50*, 2088−2097.
(30) Charcosset, C.; Juban, A.; Valour, J.-P.; Urbaniak, S.; Fessi, H. Preparation of liposomes at large scale using the ethanol injection method: Effect of scale-up and injection devices. *Chem. Eng. Res. Des.* **2015**, *94*, 508−515.
(31) Jaafar-Maalej, C.; Diab, R.; Andrieu, V.; Elaissari, A.; Fessi, H. Ethanol injection method for hydrophilic and lipophilic drug-loaded liposome preparation. *J. Liposome Res.* **2010**, *20*, 228−243.
(32) Maitani, Y. *Liposomes: Methods and Protocols, Vol. 1: Pharmaceutical Nanocarriers*; Humana Press: Totowa, NJ, 2010; pp 393−403.10.1007/978-1-60327-360-2
(33) Maitani, Y.; Igarashi, S.; Sato, M.; Hattori, Y. Cationic liposome (DC-Chol/DOPE = 1:2) and a modified ethanol injection method to prepare liposomes, increased gene expression. *Int. J. Pharm.* **2007**, *342*, 33−39.
(34) Szoka, F.; Papahadjopoulos, D. Procedure for preparation of liposomes with large internal aqueous space and high capture by reverse-phase evaporation. *Proc. Natl. Acad. Sci. U. S. A.* **1978**, *75*, 4194−4198.
(35) Jiskoot, W.; Teerlink, T.; Beuvery, E. C.; Crommelin, D. J. A. Preparation of liposomes via detergent removal from mixed micelles by dilution. *Pharm. Weekbl., Sci. Ed.* **1986**, *8*, 259−265.
(36) Yu, B.; Lee, R. J.; Lee, L. J. *Methods in Enzymology*; Academic Press, 2009; Vol. *465*; pp 129−141. 10.1016/S0076-6879(09)65007-2
(37) Traikia, M.; Warschawski, D. E.; Recouvreur, M.; Cartaud, J.; Devaux, P. F. Formation of unilamellar vesicles by repetitive freeze-thaw cycles: characterization by electron microscopy and 31 P-nuclear magnetic resonance. *Eur. Biophys. J.* **2000**, *29*, 184−195.
(38) Benjakul, R.; Panyarachun, B.; Sarisuta, N. Preparation of dry reconstituted liposomal powder by freeze-drying at room temperature. *J. Liposome Res.* **2011**, *21*, 28−37.
(39) Huang, Z.; Li, X.; Zhang, T.; Song, Y.; She, Z.; Li, J.; Deng, Y. Progress involving new techniques for liposome preparation. *Asian J. Pharm. Sci.* **2014**, *9*, 176−182.
(40) Barnadas-Rodriguez, R.; Sabes, M. Factors involved in the production of liposomes with a high-pressure homogenizer. *Int. J. Pharm.* **2001**, *213*, 175−186.
(41) Maherani, B. M.; Arab-Tehrany, E.; Mozafari, M. R.; Gaiani, C.; Linder, M. Liposomes: A Review of Manufacturing Techniques and Targeting Strategies. *Curr. Nanosci.* **2011**, *7*, 436−452.
(42) Massing, U.; Cicko, S.; Ziroli, V. Dual asymmetric centrifugation (DAC)—A new technique for liposome preparation. *J. Controlled Release* **2008**, *125*, 16−24.
(43) Tien Sing Young, R. V.; Tabrizian, M. Rapid, one-step fabrication and loading of nanoscale 1,2-distearoyl-sn-glycero-3-phosphocholine liposomes in a simple, double flow-focusing microfluidic device. *Biomicrofluidics* **2015**, *9*, 046501.
(44) Capretto, L.; Carugo, D.; Mazzitelli, S.; Nastruzzi, C.; Zhang, X. Microfluidic and lab-on-a-chip preparation routes for organic nanoparticles and vesicular systems for nanomedicine applications. *Adv. Drug Delivery Rev.* **2013**, *65*, 1496−1532.
(45) Jahn, A.; Stavis, S. M.; Hong, J. S.; Vreeland, W. N.; DeVoe, D. L.; Gaitan, M. Microfluidic Mixing and the Formation of Nanoscale Lipid Vesicles. *ACS Nano* **2010**, *4*, 2077−2087.
(46) Hood, R. R.; DeVoe, D. L. High-Throughput Continuous Flow Production of Nanoscale Liposomes by Microfluidic Vertical Flow Focusing. *Small* **2015**, *11*, 5790−5799.
(47) Davies, R. T.; Kim, D.; Park, J. Formation of liposomes using a 3D flow focusing microfluidic device with spatially patterned wettability by corona discharge. *J. Micromech. Microeng.* **2012**, *22*, 055003.
(48) Wi, R.; Oh, Y.; Chae, C.; Kim, D. H. Formation of liposome by microfluidic flow focusing and its application in gene delivery. *Korea-Australia Rheology Journal* **2012**, *24*, 129−135.
(49) Pradhan, P.; Guan, J.; Lu, D. A facile microfluidic method for production of liposomes. *Anticancer Res.* **2008**, *28*, 943−947.
(50) Carugo, D.; Bottaro, E.; Owen, J.; Stride, E.; Nastruzzi, C. Liposome production by microfluidics: potential and limiting factors. *Sci. Rep.* **2016**, *6*, 6.
(51) Michelon, M.; Oliveira, D. R. B.; de Figueiredo Furtado, G.; Gaziola de la Torre, L.; Cunha, R. L. High-throughput continuous production of liposomes using hydrodynamic flow-focusing microfluidic devices. *Colloids Surf., B* **2017**, *156*, 349−357.
(52) Reiner, J. E.; Jahn, A.; Stavis, S. M.; Culbertson, M. J.; Vreeland, W. N.; Burden, D. L.; Geist, J.; Gaitan, M. Accurate Optical Analysis of Single-Molecule Entrapment in Nanoscale Vesicles. *Anal. Chem.* **2010**, *82*, 180−188.
(53) Vogel, R.; Coumans, F. A. W.; Maltesen, R. G.; Boing, A. N.; Bonnington, K. E.; Broekman, M. L.; Broom, M. F.; Buzas, E. I.; Christiansen, G.; Hajji, N.; et al. A standardized method to determine the concentration of extracellular vesicles using tunable resistive pulse sensing. *J. Extracell. Vesicles* **2016**, *5*, 31242.
(54) Caldwell, K. D.; Williams, S. K. R. *Field-Flow Fractionation in Biopolymer Analysis*; Springer: New York, 2012; Chapter 14, pp 207−210.
(55) Matsuzaki, K.; Murase, O.; Sugishita, K.; Yoneyama, S.; Akada, K.; Ueha, M.; Nakamura, A.; Kobayashi, S. Optical characterization of liposomes by right angle light scattering and turbidity measurement. *Biochim. Biophys. Acta, Biomembr.* **2000**, *1467*, 219−226.
(56) Maas, S. L.; de Vrij, J.; van der Vlist, E. J.; Geragousian, B.; van Bloois, L.; Mastrobattista, E.; Schiffelers, R. M.; Wauben, M. H.; Broekman, M. L.; Nolte-'t Hoen, E. N Possibilities and limitations of current technologies for quantification of biological extracellular vesicles and synthetic mimics. *J. Controlled Release* **2015**, *200*, 87−96.
(57) Bhatia, S. *Natural Polymer Drug Delivery Systems*; Springer: New York, 2016; Chapter 2, pp 40−44.
(58) Malloy, A. Count, size and visualize nanoparticles. *Mater. Today* **2011**, *14*, 170−173.
(59) Hui, L.; Chen, X.; Haughey, N. J.; Geiger, J. D. Role of Endolysosomes in HIV-1 Tat-Induced Neurotoxicity. *ASN Neuro* **2012**, *4*, AN20120017.
(60) Xiao, H.; Neuveut, C.; Tiffany, H. L.; Benkirane, M.; Rich, E. A.; Murphy, P. M.; Jeang, K.-T. Selective CXCR4 antagonism by Tat: Implications for in vivo expansion of coreceptor use by HIV-1. *Proc. Natl. Acad. Sci. U. S. A.* **2000**, *97*, 11466−11471.
(61) Ohi, M.; Li, Y.; Cheng, Y.; Walz, T. Negative staining and image classification: powerful tools in modern electron microscopy. *Biol. Proced. Online* **2004**, *6*, 23−34.
(62) Crosland-Taylor, P. J. A Device for Counting Small Particles suspended in a Fluid through a Tube. *Nature* **1953**, *171*, 37−38.
(63) Knight, J. B.; Vishwanath, A.; Brody, J. P.; Austin, R. H. Hydrodynamic Focusing on a Silicon Chip: Mixing Nanoliters in Microseconds. *Phys. Rev. Lett.* **1998**, *80*, 3863−3866.
(64) Lin, B. *Microfluidics: Technologies and Applications.*, 1st ed.; Springer: Berlin, 2013. 10.1007/978-3-642-23050-9
(65) Dziubinski, M. *Hydrodynamic Focusing in Microfluidic Devices*, 1st ed.; INTECH Open Access Publisher: Rijeka, Croatia, 2012. 10.5772/34690

DOI: 10.1021/acsbiomaterials.7b00572
ACS Biomater. Sci. Eng. 2018, 4, 502−513

(66) Costa, A. P.; Xu, X.; Khan, M. A.; Burgess, D. J. Liposome Formation Using a Coaxial Turbulent Jet in Co-Flow. *Pharm. Res.* **2016**, *33*, 404−416.
(67) Hebert, C. G.; Staton, S. J. R.; Hudson, T. Q.; Hart, S. J.; Lopez-Mariscal, C.; Terray, A. Dynamic radial positioning of a hydrodynamically focused particle stream enabled by a three-dimensional microfluidic nozzle. *Biomicrofluidics* **2015**, *9*, 024106.
(68) DeCarlo, S.; Harris, J. R. Negative staining and cryo-negative staining of macromolecules and viruses for TEM. *Micron* **2011**, *42*, 117−131.
(69) Ruozi, B.; Belletti, D.; Tombesi, A.; Tosi, G.; Bondioli, L.; Forni, F.; Vandelli, M. A. AFM, ESEM, TEM, and CLSM in liposomal characterization: a comparative study. *Int. J. Nanomed.* **2011**, 557.
(70) Kastner, E.; Kaur, R.; Lowry, D.; Moghaddam, B.; Wilkinson, A.; Perrie, Y. High-throughput manufacturing of size-tuned liposomes by a new microfluidics method using enhanced statistical tools for characterization. *Int. J. Pharm.* **2014**, *477*, 361−368.
(71) Honary, S.; Zahir, F. Effect of Zeta Potential on the Properties of Nano-Drug Delivery Systems - A Review (Part 2). *Trop. J. Pharm. Res.* **2013**, *12*, 12.
(72) Filipe, V.; Hawe, A.; Jiskoot, W. Critical Evaluation of Nanoparticle Tracking Analysis (NTA) by NanoSight for the Measurement of Nanoparticles and Protein Aggregates. *Pharm. Res.* **2010**, *27*, 796−810.

DOI: 10.1021/acsbiomaterials.7b00572
ACS Biomater. Sci. Eng. 2018, 4, 502−513